Time-resolved study of the lasing emission from high vibrational levels of N_2^+ pumped with circularly polarized femtosecond pulses

Dongjie Zhou (周冬杰), Xiang Zhang (张 翔), Qi Lu (卢 琦), Qingqing Liang (梁青青), and Yi Liu (刘 一)*

Shanghai Key Laboratory of Modern Optical System, University of Shanghai for Science and Technology, Shanghai 200093, China

**Corresponding author: yi.liu@usst.edu.cn*

Received September 19, 2019; accepted November 14, 2019; posted online February 13, 2020

We experimentally investigated the forward 353.8 nm radiation from plasma filaments in pure nitrogen gas pumped by intense circularly polarized 800 nm femtosecond laser pulses. This emission line corresponds to the $B^2\Sigma_u^+(v'=4)-X^2\Sigma_g^+(v=3)$ transition of nitrogen ions. In the presence of an external seeding pulse, the 353.8 nm signal was amplified by 3 orders of magnitude. Thanks to the much enhanced intensity, we performed time-resolved measurement of the amplified 353.8 nm emission based on the sum-frequency generation technique. It was revealed that the built-up time and duration of these emissions are both inversely proportional to the gas pressure, while the radiation peak power grows up nearly quadratically with pressure, indicating that the 353.8 nm radiation is of the nature of superradiance.

Keywords: femtosecond pulses; plasma; nitrogen ions; superradiance; time-resolved measurement.
doi: 10.3788/COL202018.023201.

Cavity-free air lasing pumped by ultrafast laser pulses has attracted much attention in recent years due to its unique properties[1–12]. First, bidirectional air lasing occurs without any external optical cavity due to a high single pass optical gain. Second, the gain media are ambient air (N_2, O_2, Ar) or their derivatives under laser excitation, which is ubiquitous. Finally, air lasing can be potentially generated far away from the pump laser system, since the intensity of the driven ultrafast pulses can easily reach 10^{13}–10^{14} W/cm^2 even a kilometer away thanks to the filamentation process[13–16]. Because of the above characteristics, air lasing holds great potential in optical remote sensing applications, which has been demonstrated in recent studies[17,18]. At present, most studies of air lasing are focused on the lasing action of atomic oxygen (O)[1,10], argon atom[12], neutral nitrogen molecules (N_2)[4,8,19,20], as well as ionic nitrogen molecules (N_2^+)[2,5–7,11]. Up to now, the physical mechanisms of the lasing effect of O, Ar, N_2 are more or less understood[1,4,8,10,12]. In contrast, the lasing of nitrogen ions exhibits very rich phenomena under different pumping conditions, and its mechanism is still unclear[2,5–7,21–23].

Most studies on nitrogen ion lasing are focused on the 391.4 nm and 427.8 nm emission lines, which correspond to the optical transition between $B^2\Sigma_u^+(v'=0)$ and $X^2\Sigma_g^+(v=0,\,1)$ states, respectively, where the v' and v denote the vibrational quantum levels of the upper and lower electronic states[2,5–7]. These two emission lines can be readily produced by an 800 nm pulse with moderate pulse energy (~1 mJ), with a focusing geometry of NA ~0.02–0.03 commonly used by different research groups[6,7,11]. To identify the nature of this radiation, the temporal profile of these emissions has been studied for different gas pressure p and plasma length with the time-resolved method[22,24]. It was found that the built-up time and the pulse duration both scale with p^{-1}, while the radiation peak power grows with p^2, indicating that the 391.4 nm emission is superradiance[22,24]. In the experiments, linearly polarized pump pulses were usually employed. With an increase of pump pulse ellipticity, it has been observed that the forward lasing signal drops significantly[22,25,26]. For circularly polarized pump pulses, no forward 391.4/427.8 nm signal or a much weaker one has been observed[22,25,26]. Surprisingly, Zhai *et al.* recently reported that with intense circularly polarized 800 nm pulses, coherent forward emission at 353.3, 353.8, and 354.9 nm can be generated. This emission stems from the $B^2\Sigma_u^+(v'=5,\,4,\,3)$ to $X^2\Sigma_g^+(v=4,\,3,\,2)$ transition, i.e., the highly excited state of nitrogen ions[27,28]. With external injected seeding pulses, strong optical amplification has been observed, and the gain dynamics have been measured[27,28]. Up to now, to the best of our knowledge, the temporal profile of this emission has not been characterized, and its mechanism remains unclear.

In this study, we report on time-resolved measurement of the seeded 353.8 nm radiation from nitrogen gas plasma pumped by intense circularly polarized 800 nm femtosecond pulses. To identify the optimal experimental conditions, we first investigated the pump laser ellipticity and pressure dependence of the 353.8 nm emission. In the presence of an external seeding pulse at proper conditions, a spectrum amplification by 3 orders of magnitude was obtained. With the much enhanced emission energy, we were able to characterize it in the temporal domain with nonlinear sum-frequency generation (SFG) method.

It was found that the pulse built-up time τ_d and the pulse duration τ_w are inversely proportional to the nitrogen pressure p, while the pulse peak power increases almost quadratically with p. Based on these characteristic features, we come to the conclusion that the 353.8 nm lasing radiation from the high vibrational levels of N_2^+ is superradiance.

In the experiment, the femtosecond laser pulse (35 fs, 1 kHz) from a Ti:sapphire amplification system at the 796 nm wavelength has a maximum pulse energy of 11 mJ. The experimental setup is schematically shown in Fig. 1. The output pulses were split sequentially into three parts with two beam splitters, denoted as pump, seed, and probe pulses in the figure. The energy of the main pump pulses was 7 mJ, and a quarter wave-plate (QWP, Thorlabs, WPQ10M-808) was installed on this beam path to change its polarization from linearly to circularly polarized states. For the generation of the seed pulse with the spectral component around 353.8 nm, the 796 nm pulses first pass through a second harmonic generation beta barium borate (BBO) crystal to produce laser pulses around 398 nm. The second harmonics pulses were focused into a 3 mm thick fused silica sample to broaden its spectrum through the self-phase-modulation effect. We used interference filters with a bandwidth of 10 nm to select the required spectral component around 353.8 nm from the broadened white-light spectrum. The pump and the seed pulse were combined by a dichroic mirror (DM) and then focused with an $f = 50$ cm lens into a gas chamber filled with pure nitrogen gas.

The third 796 nm pulse (probe) was combined with the forward 353.8 nm radiation from the gas plasma by another DM, focused by an $f = 100$ mm lens onto an SFG BBO crystal cut at 44.3°. The SFG signal around 246 nm was spectrally filtered out from the residual 353.8 nm and 796 nm radiation with proper optical filters (BG 11 and interference filter around 250 nm with 10 nm bandwidth) and collected into a fiber spectrometer. The seed and the probe pulse were equipped with high-precision mechanical optical delay lines, so that the time delay between the three pulses can be adjusted separately.

We first measured the forward lasing signal as a function of pump pulse polarization with only the pump pulse. The results are presented in Fig. 2. The polarization of the pump pulse was changed by rotation of the QWP, where

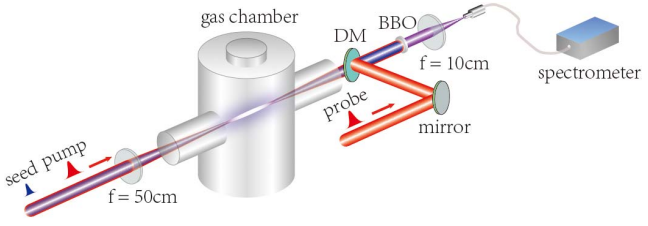

Fig. 1. Schematic experimental setup. Beam splitters (not shown) separated the laser pulses into three pulses, denoted as the pump, seed, and probe. The forward 353.8 nm radiation was recombined with the probe pulse by a dichroic mirror (DM).

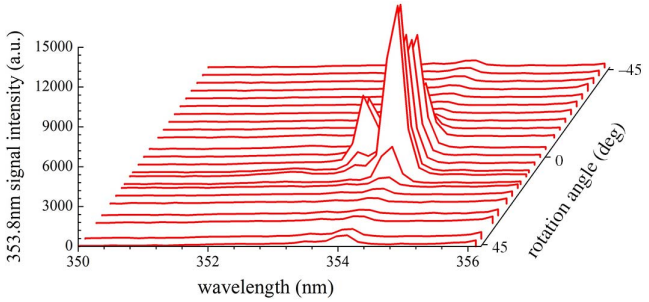

Fig. 2. Dependence of 353.8 nm signal intensity as a function of the rotation angle of the quarter wave-plate. The angles 0° and 45° correspond to circular polarization and linear polarization, respectively.

0° and 45° represent circular polarization and linear polarization, respectively. With circularly polarized 796 nm pump pulses, a strong emission at 353.8 nm and a relatively weaker peak at 353.5 nm were observed. The signal drops down rapidly for polarization deviated from the circular state, in agreement with previous reports[27,28].

We then injected an external seeding pulse inside the nitrogen gas plasma, and the experimental results are shown in Fig. 3. It should be noted that in Fig. 3 the spectra of the seeding pulse and the 353.8 nm emission obtained without the seeding pulse have been multiplied by a factor of 100 for easy comparison. With both pump and seeding pulses, the 353.8 nm signal was strongly enhanced. Compared to the spectral intensity of the seeding pulse at 353.8 nm, an amplification factor of 3200 was obtained. Considering a plasma length of 15 mm, we estimated the optical gain to be $g = \ln(I_f/I_0)/l = 5.38\,\mathrm{cm}^{-1}$.

We further investigated the 353.8 nm signal intensity as a function of nitrogen gas pressure in both cases without and with the seeding pulses. As can be seen in Fig. 4, similar pressure dependence was observed for the two cases, with an optimal pressure around 90 mbar in our current experiments.

Furthermore, we investigated gain dynamics of the 353.8 nm transition for different gas pressures. In the

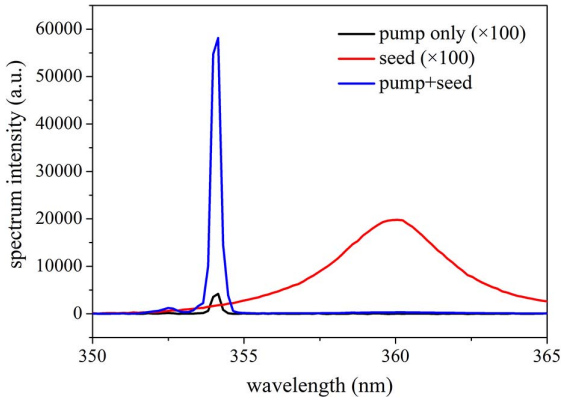

Fig. 3. Amplified spectra of the seed pulse inside nitrogen plasma. The spectrum of seed pulse and that from pump pulse are also presented, multiplied by a factor of 100 for visibility.

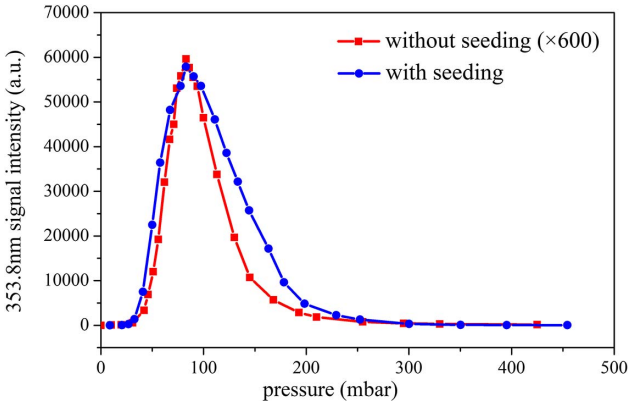

Fig. 4. Dependence of 353.8 nm signal intensity on gas pressure without seeding and with seeding.

experiments, we measured the intensity of the amplified 353.8 nm as a function of the time delay between the pump pulse and seed pulse. As shown in Fig. 5, the lasing signal reaches its maximum of 0–500 fs after the pump pulse and decreases gradually up to delay of ~5 ps. Importantly, it should be noticed that the rising edge of the signal, i.e., the establishment of the optical gain, is independent of the gas pressure. This observation is distinct from the lasing action of N_2, where the optical gain is established in 5–10 ps and depends sensitively on the gas pressure[19,20]. In the lasing process of N_2 pumped by intense circularly polarized 800 nm femtosecond pulses, the mechanism for optical gain formation was attributed to population inversion between the $C^3\Pi_u$ and $B^3\Pi_g$ states based on electron–molecule collision excitation[8,19,20]. The mean collision time between electron and N_2 is on the order of a fraction of a picosecond for electron energy of >11 eV at standard temperature and pressure (STP) conditions. Therefore, a gain formation time of several picoseconds can be expected since many collision events are necessary to result in population inversion. In the meantime, the gain formation time depends on the gas pressure, because the mean collision time decreases for higher pressure. Here, the sub-picosecond formation time of the optical gain at 353.8 nm and its independence on gas pressure indicate that the pressure-dependent electron–molecule collision cannot be the physical mechanism for optical gain formation.

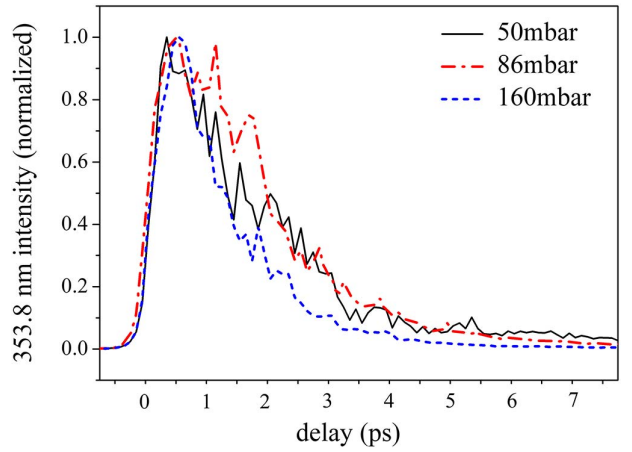

Fig. 5. Dependence of 353.8 nm signal intensity on the time delay between the pump and seed pulses for different gas pressures.

The pressure-independent sub-picosecond formation time of the optical gain at 353.8 nm is actually similar to that of the 391.4 nm lasing action[6,22], except that for 391.4 nm emission generation linearly polarized pump pulses are much more efficient than circular polarization. With the mechanism for optical gain at 391.4 nm intensively debated nowadays[2,5–7,21–23], the underlying physics for the optical gain at 353.8 nm is also unclear, which requires further study.

Nevertheless, we were able to perform time-resolved measurement of the radiation based on SFG of the 353.8 nm radiation and the weak 800 nm probe pulse, since the intensity of the 353.8 nm radiation has been enhanced by 3 orders of magnitude by injection of a seeding pulse (Fig. 3). In the experiments, we recorded the SFG signal at 246 nm for varying time delays between the 353.8 nm signal and the probe pulse, which reflects the temporal profile of the 353.8 nm lasing signal. The experimental results for different gas pressures are shown in Fig. 6(a). The pump pulse was 500 fs precedent with respect to the seeding pulse, and the zero delay was defined as the temporal position of the seeding pulse. The small peaks at zero delay correspond to the seeding pulse, which is not amplified. The amplified pulse energy actually lags behind the seeding pulse by a few picoseconds, with its peaks advancing

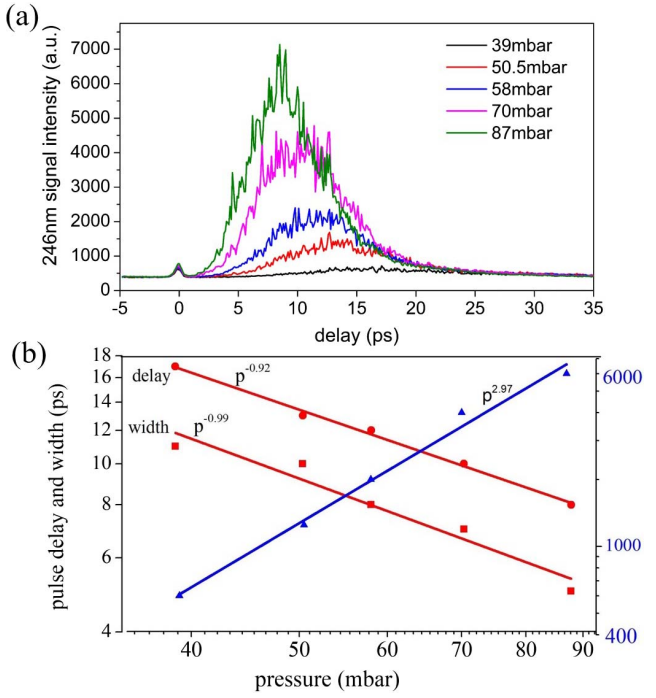

Fig. 6. (a) Temporal profile of the amplified 353.8 nm signal for different gas pressures. (b) Dependence of pulse delay, pulse width, and peak intensity on gas pressure.

toward the seeding pulse for higher gas pressure. In Fig. 6(b), we present the dependence of the pulse built-up time τ_d, the pulse duration τ_w, and the peak power on the gas pressure. It is seen that both τ_d and τ_w are inversely proportional to the gas pressure (p^{-1}), while the peak power scales up with a dependence of $p^{2.9}$, pointing out that the 353.8 nm emission is of the nature of superradiance. We noticed that the peak power scales up faster than the quadratic dependence expected for superradiance, which was also observed for the 391.4 nm emission[22]. This can be due to that for higher gas pressure the self-generated white-light continuum shifts gradually toward the short-wavelength side and starts to serve as the seeding pulse, which further accelerates the superradiant radiation process.

Why does the 353.8 nm emission manifest as superradiance, like the 391.4 nm radiation obtained with linearly polarized pump pulses? It is known that in gain media, superradiant emission can develop if the polarization evolves faster than or on the same time scale as the decoherence time[9,29]. The average Rabi frequency can be estimated by $\Omega = D_{\mathrm{BX}}E/h$, where D_{BX} is the electric dipole moment, and E is the electric field amplitude. The electric dipole moment D_{BX} is found to be $D_{\mathrm{BX}} = 2\,D = 6.66 \times 10^{-30}\,\mathrm{C}\cdot\mathrm{m}$[5]. The electric field is estimated in the following manner. Considering the measured pulse energy of ∼100 nJ, the pulse duration of ∼10 ps, and the diameter of the gain area of ∼100 μm, the average intensity of the 353.8 nm radiation was found to be $I = 1.27 \times 10^9\,\mathrm{W/cm^2}$. The corresponding electric field was then calculated to be $E = 1.04 \times 10^6\,\mathrm{V/m}$. Based on the experimentally measured parameters, we estimated the Rabi frequency for the 353.8 nm transition to be $\Omega = 7.06 \times 10^9\,\mathrm{rad/s}$. For nitrogen gas of ∼50 mbar, the molecule–molecule collision frequency is about $2 \times 10^8\,\mathrm{rad/s}$. Therefore, the upper limit for the collision dephasing rate is set to be $2 \times 10^8\,\mathrm{rad/s}$. We can see that the average Rabi frequency is much higher than the dephasing rate, and molecular coherence effects will occur, which leads to superradiant emission in our case. This reasoning also applies to the case of 391.4 nm emission, where its intensity is higher than or on the same order as that of the 353.8 nm emission. Since the femtosecond pulses establish the optical gain for 353.8 nm (circularly polarized pump) or 391.4 nm (linearly polarized pump) in an ultrashort time window determined by its duration, the development of the superradiant emission on the time scale of tens of picoseconds is expected to be independent on the pump pulse polarization.

In conclusion, we have performed a time-resolved study of the forward 353.8 nm emission from high vibrational levels of N_2^+ pumped by intense circularly polarized femtosecond laser pulses. With the pump-probe method, it was found that the optical gain is established in less than 500 fs, independent of the gas pressure. This suggests that a photonics process, instead of an electron collision excitation, is responsible for the creation of optical gain. Spectral amplification by 3 orders of magnitude was observed by injection of an external seeding pulse, which enables a time-resolved measurement based on the SFG technique. We found that the amplified 353.8 nm signal exhibits characteristic dependence on nitrogen gas pressure, with pulse built-up time τ_d and pulse duration τ_w scaling with p^{-1} and radiation peak power scaling with $p^{2.9}$. Based on these characteristic features, we came to the conclusion that the 353.8 nm emission is of the nature of superradiance.

The work was supported in part by the National Natural Science Foundation of China (Nos. 11574213 and 11904232), Innovation Program of Shanghai Municipal Education Commission (No. 2017-01-07-00-07-E00007), and the Shanghai Municipal Science and Technology Commission (No. 17060502500). Y. Liu acknowledges the support of the Program for Professor of Special Appointment (Eastern Scholar) at the Shanghai Institutions of Higher Learning (No. TP2014046).

References

1. A. Dogariu, J. B. Michael, M. O. Scully, and R. B. Miles, Science **331**, 442 (2011).
2. J. Yao, B. Zeng, H. Xu, G. Li, W. Chu, J. Ni, H. Zhang, S. L. Chin, Y. Cheng, and Z. Xu, Phys. Rev. A **84**, 051802(R) (2011).
3. S. L. Chin, H. Xu, Y. Cheng, Z. Xu, and K. Yamanouchi, Chin. Opt. Lett. **11**, 013201 (2013).
4. D. Kartashov, S. Ališauskas, G. Andriukaitis, A. Pugžlys, M. Shneider, A. Zheltikov, S. L. Chin, and A. Baltuška, Phys. Rev. A **86**, 033831 (2012).
5. H. Xu, E. Lotstedt, A. Iwasaki, and K. Yamanouchi, Nat. Commun. **6**, 8347 (2015).
6. J. Yao, G. Li, C. Jing, B. Zeng, W. Chu, J. Ni, H. Zhang, H. Xie, C. Zhang, H. Li, H. Xu, S. L. Chin, Y. Cheng, and Z. Xu, New J. Phys. **15**, 023046 (2013).
7. Y. Liu, Y. Brelet, G. Point, A. Houard, and A. Mysyrowicz, Opt. Express **21**, 22791 (2013).
8. S. Mitryukovskiy, Y. Liu, P. Ding, A. Houard, and A. Mysyrowicz, Opt. Express **22**, 12750 (2014).
9. A. J. Traverso, R. Sanchez-Gonzalez, L. Yuan, K. Wang, D. V. Voronine, A. M. Zheltikov, Y. Rostovtsev, V. A. Sautenkov, A. V. Sokolov, S. W. North, and M. O. Scully, Proc. Natl. Acad. Sci. U.S.A. **109**, 15185 (2012).
10. A. Laurain, M. Scheller, and P. Polynkin, Phys. Rev. Lett. **113**, 253901 (2014).
11. M. Lei, C. Wu, A. Zhang, Q. Gong, and H. Jiang, Opt. Express **25**, 4535 (2017).
12. A. Dogariu and R. B. Miles, Opt. Express, **24**, A544 (2016).
13. A. Couairon and A. Mysyrowicz, Phys. Rep. **441**, 47 (2007).
14. S. L. Chin, S. A. Hosseini, W. Liu, Q. Luo, F. Théberge, N. Aközbek, A. Becker, V. P. Kandidov, O. G. Kosareva, and H. Schroeder, Can. J. Phys. **83**, 863 (2005).
15. M. Durand, A. Houard, B. Prade, A. Mysyrowicz, A. Durecu, B. Moreau, D. Fleury, O. Vasseur, H. Borchert, K. Diener, R. Schmitt, F. Théberge, M. Chateauneuf, J. F. Daigle, and J. Dubois, Opt. Express **21**, 26836 (2013).
16. Z. Zhu, T. Wang, Y. Liu, N. Chen, H. Zhang, H. Sun, H. Guo, J. Zhang, X. Zhang, G. Li, C. Liu, Z. Zeng, J. Liu, S. L. Chin, R. Li, and Z. Xu, Chin. Opt. Lett. **16**, 073201 (2018).

17. P. N. Malevich, D. Kartashov, Z. Pu, S. Alisauskas, A. Pugzlys, A. Baltuska, L. Giniunas, R. Danielius, A. A. Lanin, A. M. Zheltikov, M. Marangoni, and G. Cerullo, Opt. Express, **20**, 18784 (2012).
18. P. N. Malevich, R. Maurer, D. Kartashov, S. Ališauskas, A. A. Lanin, A. M. Zheltikov, M. Marangoni, G. Cerullo, A. Baltuška, and A. Pugžlys, Opt. Lett. **40**, 2469 (2015).
19. P. J. Ding, E. Oliva, A. Houard, A. Mysyrowicz, and Y. Liu, Phys. Rev. A **94**, 043824 (2016).
20. J. Yao, H. Xie, B. Zeng, W. Chu, G. Li, J. Ni, H. Zhang, C. Jing, C. Zhang, H. Xu, Y. Cheng, and Z. Xu, Opt. Express **22**, 19005 (2014).
21. J. Yao, S. Jiang, W. Chu, B. Zeng, C. Wu, R. Lu, Z. Li, H. Xie, G. Li, C. Yu, Z. Wang, H. Jiang, Q. Gong, and Y. Cheng, Phys. Rev. Lett. **116**, 143007 (2016).
22. Y. Liu, P. Ding, G. Lambert, A. Houard, V. Tikhonchuk, and A. Mysyrowicz, Phys. Rev. Lett. **115**, 133203 (2015).
23. H. Li, M. Hou, H. Zang, Y. Fu, E. Lötstedt, T. Ando, A. Iwasaki, K. Yamanouchi, and H. Xu, Phys. Rev. Lett. **122**, 013202 (2019).
24. G. Li, C. Jing, B. Zeng, H. Xie, J. Yao, W. Chu, J. Ni, H. Zhang, H. Xu, Y. Cheng, and Z. Xu, Phys. Rev. A **89**, 033833 (2014).
25. H. Zhang, C. Jing, G. Li, H. Xie, J. Yao, B. Zeng, W. Chu, J. Ni, H. Xu, and Y. Cheng, Phys. Rev. A **88**, 063417 (2013).
26. M. Britton, P. Laferrière, D. H. Ko, Z. Li, F. Kong, G. Brown, A. Naumov, C. Zhang, L. Arissian, and P. B. Corkum, Phys. Rev. Lett. **120**, 133208 (2018).
27. C. Jing, J. Yao, Z. Li, J. Ni, B. Zeng, W. Chu, G. Li, H. Xie, and Y. Cheng, J. Phys. B: At. Mol. Opt. Phys. **48**, 094001 (2015).
28. K. Zhai, Z. Li, H. Xie, C. Jing, G. Li, B. Zeng, W. Chu, J. Ni, J. Yao, and Y. Cheng, Chin. Opt. Lett. **13**, 050201 (2015).
29. L. Yuan, B. H. Hokr, A. J. Traverso, D. V. Voronine, Y. Rostovtsev, A. V. Sokolov, and M. O. Scully, Phys. Rev. A **87**, 023826 (2013).